TECHNICAL UNIVERSITY OF CLUJ-NAPOCA

ACTA TECHNICA NAPOCENSIS

Series: Applied Mathematics, Mechanics, and Engineering
Vol. 67, Issue Special IV, August, 2024

CLEARANCE OPTIMIZATION FOR ROLLER-SHOE TRANSMISSION MECHANISM FROM DIESEL HIGH-PRESSURE COMMON RAIL PUMPS

Razvan-Constantin IORDACHE, Carmen BUJOREANU, Dumitru OLARU

Abstract: *The roller-shoe drive mechanism is the most important subassembly of the high-pressure pump and it can be severely affected by the wear. The diametral clearance between the mechanical components in direct contact is a parameter that can have a decisive influence on the wear process and also on the lifetime of the assembly. The purpose of our paper is to perform an analytical calculation in order to highlight a range of values of the clearance between the roller and the shoe, where the high-pressure pump can run safely without components damaging. The results are experimentally validated.*

Key words: *high-pressure pump, roller-shoe transmission, clearance.*

1. INTRODUCTION

Motion transmission in high-pressure pumps is achieved by classic mechanisms, such as shoe-rollers or cam follower [1]. The roller-shoe drive mechanism is a sub-assembly of simple construction and it is used in modern high-pressure pumps, being capable of high performance at low cost [2]. The cylindrical roller is characterized by a design adaptable to a wide range of assemblies. Its use offers the advantage of improved load transmission for heavy weights and faster operation compared to alternative designs [3]. The shoe is tailored to suit mounting requirements and has a cylindrical inner surface that ensures even contact with the roller. Thus, when it comes to the occurrence and reduction of wear, several key parameters will be monitored, such as maximum applied load, lubricant film thickness, relative surface clearance, surface conditions and lubricant temperature. The subject of our paper focus on the clearance between the two elements. Generally, the clearance between components is a critical parameter that can significantly impact the lifespan of the assembly to which it belongs [4]. The most relevant examples, presenting similar conditions to the operation of the roller-shoe system, can be found in bearings. The clearance has a direct impact on the lubrication regimes between the two components, the heating of the components and especially on the stability of the components during their motion [5]. Hence, a positive step in this regard involves identifying an optimal clearance value to ensure that the possible wear of the contacting components is not affected by this.

The calculation is based on information found in the literature applicable to cylindrical roller bearings. They are basic components for mechanical transmissions and the proper distribution of applied loads is a key element in terms of service life [6]. The directions of load application in cylindrical roller bearings are similar to those in the roller-shoe mechanism. Also, the evolution of the transition between lubrication regimes follows a similar path [7]. Considering the magnitude of effort involved, ensuring an appropriate clearance between components helps maintain a constant thickness of the lubricant film. Analyzing the calculation models of the clearance in the literature, we followed a specific algorithm that can be adapted on the roller-shoe mechanism [8]. It requires knowledge of the dimensional values of the components, the operating conditions of the mechanism and some lubrication parameters. The result of the calculation leads to obtaining a range of clearance values in which the mechanism can safely operate. The experimental validation was carried out by endurance tests. In order to accomplish this, two roller-shoe mechanisms, each featuring the minimum and maximum clearance values within the calculated range, are selected and installed on high-pressure pumps. These mechanisms undergo a Low Sommerfeld test, exposing them to aggravating operating conditions [9]. After the test, the condition of the components with the optimal calculated clearance is thus highlighted, confirming the theoretical approach.

2. ROLLER-SHOE MECHANISM DIMENSIONAL CHARACTERISTICS

The roller-shoe assembly, in a first approximation, can be considered as a cylinder inside another cylinder. Figure 1 shows the main dimensional features of a roller-shoe drive mechanism from a high-pressure functional pump. The dimensional values were acquired through measurements conducted after the secure disassembly of the components [10].

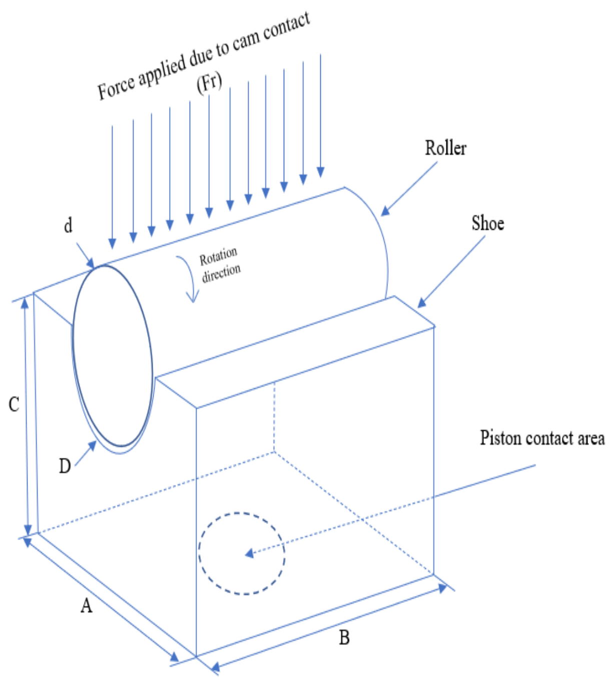

Fig. 1. Roller-shoe mechanism representation [10]

Table 1 contains the main dimensions of the transmission mechanism components. These can be used to obtain real clearance values following specific calculations. The components come from a used pump, in very good condition.

Table 1

The measured dimensions of the components.

Dimension/Symbol	Measured value	Measurement unit
Roller diameter (d)	12.029	mm
Shoe diameter (D)	12.050	
Shoe/roller length (B)	21	
Shoe width (A)	17	
Shoe height (C)	15	

3. ROLLER-SHOE CLEARANCE CALCULATION

The calculation of an optimal clearance between the roller and shoe is one of the important solutions to reduce the mechanism wear and increase the components life. In order to have applicability in the industrial field, it is necessary that these values fall within a range. Thus, the purpose of this optimization calculation is to highlight a range of values of the clearance between the roller and the shoe, where the high-pressure pump can operate safely, without damaging the components due to inadequate clearance. The calculation algorithm follows some basic steps identified in the literature [8]. They are adapted according to the geometry of the roller-shoe mechanism. The clearance optimization is performed based on imposed operating and lubrication parameters. The specified parameter values result from the calculation of the mechanism in a predominantly mixed lubrication regime, reflecting its prevailing operating conditions [10]. Thus, we use as initial data the parameters from Table 2.

Table 2

The value of the imposed parameters

Parameter/Symbol	Imposed Value	Measurement unit
Roller speed (n)	114.3	rot/sec
Minimum lubricant film thickness (h_{min})	0.735	μm
Radial force (Fr)	6051.38	N
Fluid inlet temperature (T_i)	60	°C
Fluid specific heat (cL)	1880	$[\frac{N \cdot m}{Kg \cdot {}^{o}C}]$
Fluid density (ρL)	900	$[Kg/m^3]$

The calculation steps for the optimization of the clearance between the roller and shoe lead to obtaining a range of the diametral clearance optimal values.

3.1 Values selection for relative clearance (Ψ)

The choice of values for the relative clearance (diametral clearance reported to roller diameter) is made taking into account its variation range (0.0003...0.003) [8]. This interval was established in the literature based on similar conditions to those encountered in our case, having great applicability in the field of sliding bearings. To simplify this calculation and adapt it to our situation, a range of six values was chosen. The ends of the range represent the minimum and maximum clearance values identified on the roller-shoe mechanism prior to optimization. These can be found in Table 3.

Table 3

Relative clearance selected values

Ψ_1	Ψ_2	Ψ_3	Ψ_4	Ψ_5	Ψ_6
0.00099	0.0015	0.00175	0.002	0.0025	0.0029

3.2 Temperatures range selection

The temperatures range has two limits, the temperature of the working environment (T_0=60°C) and the maximum operating temperature (T_{max}=90ºC). In Table 4 we present the selected values within this range.

Table 4

The chosen values for temperature, T

T1 (°C)	T2 (°C)	T3 (°C)	T4 (°C)	T5 (°C)	T6 (°C)
60	65	70	75	80	85

3.3 Determination of lubricant viscosity, η, at selected temperatures

The choice of high-pressure pump fuel viscosity value (Diesel), as a function of temperature, uses the diagram in Fig. 2 (graphically highlighted in comparison with two other types of biofuels detailed in reference [11]) and are listed in Table 5.

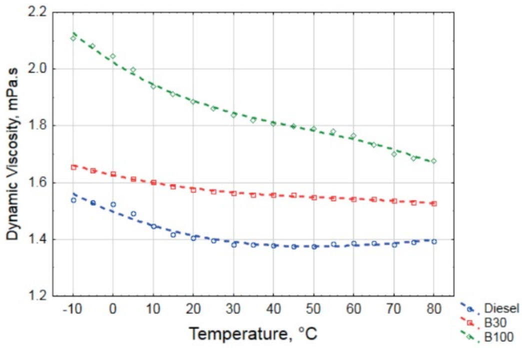

Fig. 2. Dependence between temperature and dynamic viscosity [11]

Table 5

Viscosity values η for Diesel fluid determined as a function of temperature (Pa·s) according to Figure 2

η_1	η_2	η_3	η_4	η_5	η_6
60 ºC	**65 ºC**	**70 ºC**	**75 ºC**	**80 ºC**	**85 ºC**
0.00138	0.001385	0.00139	0.001395	0.0014	0.0014

3.4 Sommerfeld Number, $S_{\Psi T}$, calculation for each combination created by relative clearance and temperature

The relation used to obtain the Sommerfeld Number is [8]:

$$S_{\Psi T} = \frac{\eta_i * n}{p_m * {\Psi_i}^2} = \frac{\eta_i * n}{\frac{F_r}{B \cdot D} * {\Psi_i}^2} \tag{1}$$

The calculated values for Sommerfeld Number, $S_{\Psi T}$, are listed in Table 6.

Table 6

Sommerfeld Number, $S_{\Psi T}$, calculated values

	$S_{\Psi T}$					
	Ψ_1	Ψ_2	Ψ_3	Ψ_4	Ψ_5	Ψ_6
T_1	0.034	0.015	0.011	0.008	0.005	0.004
T_2	0.034	0.015	0.011	0.008	0.005	0.004
T_3	0.034	0.015	0.011	0.008	0.005	0.004
T_4	0.034	0.015	0.011	0.008	0.005	0.004
T_5	0.034	0.015	0.011	0.008	0.005	0.004
T_6	0.034	0.015	0.011	0.008	0.005	0.004

3.5 Calculation of power dissipated by friction, P_f

The calculation of the power dissipated by friction is carried out using relation (2) [8].

$$P_f = C_f \cdot F_r \cdot n \cdot \pi \cdot \Psi_i \cdot \mathrm{d} \tag{2}$$

The friction coefficient (C_f) related to the relative clearance is calculated according to the Sommerfeld Number, $\mathbf{S_{\Psi T}}$. Although the shoe does not have the shape of a complete cylinder, the calculations are performed approximately at the value of π, using the relation (3) [8].

$$C_f = 2 \cdot \pi^2 \cdot S_{\Psi,T} \qquad (3)$$

The calculated values for the friction coefficient according to relation (3) are expressed in Table 7.

Table 7

Friction coefficients, C_f, according to Sommerfeld Number $S_{\Psi T}$ values

Cf					
0.335	0.148	0.108	0.079	0.049	0.039
0.335	0.148	0.108	0.079	0.049	0.039
0.335	0.148	0.108	0.079	0.049	0.039
0.335	0.148	0.108	0.079	0.049	0.039
0.335	0.148	0.108	0.079	0.049	0.039
0.335	0.148	0.108	0.079	0.049	0.039

The calculated values for the power dissipated by friction, P_f, are in Table 8.

Table 8

Calculated values for power dissipated by friction, P_f

Pf (W)						
	Ψ_1	Ψ_2	Ψ_3	Ψ_4	Ψ_5	Ψ_6
T_1	67.17	44.96	38.28	32.00	24.81	22.91
T_2	67.17	44.96	38.28	32.00	24.81	22.91
T_3	67.17	44.96	38.28	32.00	24.81	22.91
T_4	67.17	44.96	38.28	32.00	24.81	22.91
T_5	67.17	44.96	38.28	32.00	24.81	22.91
T_6	67.17	44.96	38.28	32.00	24.81	22.91

3.6 Calculation of the heat flow taken up by the lateral leakage, Pc

This calculation is carried out taking into account the fact that the heat evacuation is through the lubricant. Thus, the relation (4) is used [8]:

$$P_c = Q_s \cdot C_L \cdot \rho_L \cdot (T - T_i) \qquad (4)$$

T_i represents the inlet temperature of the fluid and T represents the value of each temperature chosen from Figure 4.

The leakage flow, Q_S, through shoe lateral sides is calculated with relation (5) [8]:

$$Q_s = C_{Qs} \cdot D^2 \cdot B \cdot n \cdot \Psi \qquad (5)$$

The lateral side leakage flow coefficient C_{Qs} is chosen from the Fig. 3 [12], depending on the B/D ration and Sommerfeld Number ($S_{\Psi T}$), and its values are presented in Table 9.

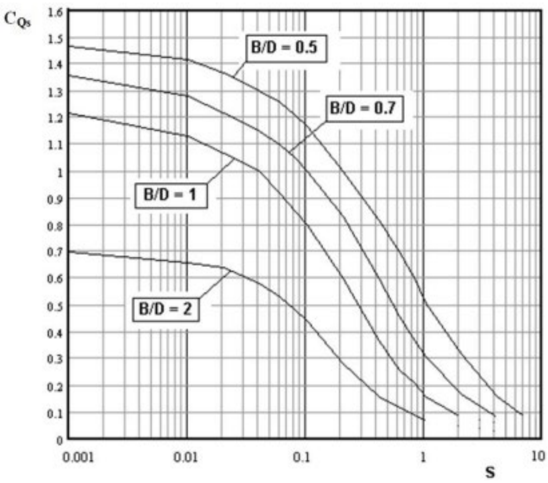

Fig. 3. Side leakage flow coefficient as a function of B/D ration and S [12]

Table 9

Values of the lateral side leakage flow coefficient, C_{Qs}, chosen according to $S_{\Psi T}$ and B/D

Cqs					
0.65	0.68	0.7	0.72	0.75	0.76
0.65	0.68	0.7	0.72	0.75	0.76
0.65	0.68	0.7	0.72	0.75	0.76
0.65	0.68	0.7	0.72	0.75	0.76
0.65	0.68	0.7	0.72	0.75	0.76
0.65	0.68	0.7	0.72	0.75	0.76

With all these calculation information, the calculated values of the leakage flow through the side areas of the shoe are given in Table 10.

Table 10

Leakage flow values Qs through the lateral of the shoe

$Q_s \cdot 10^6\ [\frac{m^3}{s}]$					
1,413	2,24	2,69	3,162	4,117	4,839
1,413	2,24	2,69	3,162	4,117	4,839
1,413	2,24	2,69	3,162	4,117	4,839
1,413	2,24	2,69	3,162	4,117	4,839
1,413	2,24	2,69	3,162	4,117	4,839
1,413	2,24	2,69	3,162	4,117	4,839

The values for the heat flow Pc calculated as a function of temperature can be found in Table 11.

Table 11

Calculated heat flux values, Pc

Pc (W)					
0	18.946	45.509	80.244	139.312	204.696
0	18.946	45.509	80.244	139.312	204.696
0	18.946	45.509	80.244	139.312	204.696
0	18.946	45.509	80.244	139.312	204.696
0	18.946	45.509	80.244	139.312	204.696
0	18.946	45.509	80.244	139.312	204.696

3.7 Heat flow variation as a function of temperature

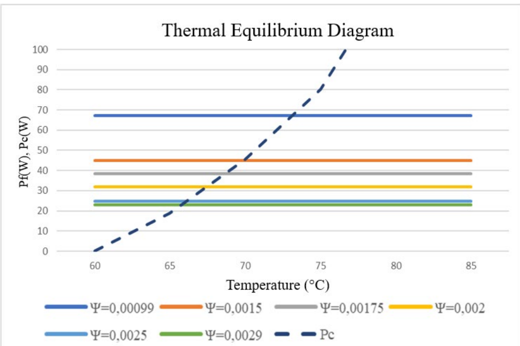

Fig. 4. Identification of equilibrium temperatures

The thermal equilibrium ,T_e, is graphically represented in Fig. 4 at the curves intersection of the power dissipated by friction and heat flow. From this graph we can extract the fluid safety temperature for each of the relative clearances. Also, depending on these, we extracted the related viscosities (Table 12).

Table 12

Values from thermal equilibrium Te, and viscosity η (Diesel fuel)

Ψ	**Te (°C)**	**η (Pa·s)**
0.00099	74	0.00138
0.0015	70	0.00138
0.00175	68	0.00138
0.002	67	0.00138
0.0025	66	0.00138
0.0029	65	0.00138

3.8 Calculation of Sommerfeld Number corresponding to equilibrium temperatures

Considering the new temperatures from the equilibrium zones, the Sommerfeld Number is recalculated for each of them. Viscosity keeps constant values, which is why we note that the recalculated values of Sommerfeld Number from Table 13 does not differ from the initial ones.

Table 13

Recalculated Sommerfeld Number values, $S_{\Psi,T}$

$S_{\Psi,T\ recalculated}$						
T	**Ψ_1**	**Ψ_2**	**Ψ_3**	**Ψ_4**	**Ψ_5**	**Ψ_6**
74	0.034	0.015	0.011	0.008	0.005	0.004
70	0.034	0.015	0.011	0.008	0.005	0.004
68	0.034	0.015	0.011	0.008	0.005	0.004
67	0.034	0.015	0.011	0.008	0.005	0.004
66	0.034	0.015	0.011	0.008	0.005	0.004
65	0.034	0.015	0.011	0.008	0.005	0.004

3.9 Calculation of the lubricant film minimum thickness for each clearance value [8]

$$h_{min\Psi} = \delta \cdot \frac{J}{2} = \delta \cdot \frac{\Psi_i \cdot d}{2} \tag{6}$$

Obtaining the variation of the minimum relative thickness δ of the lubricant film according to the recalculated Sommerfeld Number ($S_{\Psi,T}$) and the B/D ratio is carried out based on the diagram depicted in Fig. 5 [12]. The values can be found in Table 14.

Table 14

Minimum relative thickness variation values

δ					
0.18	0.1	0.07	0.06	0.035	0.02
0.18	0.1	0.07	0.06	0.035	0.02
0.18	0.1	0.07	0.06	0.035	0.02
0.18	0.1	0.07	0.06	0.035	0.02
0.18	0.1	0.07	0.06	0.035	0.02
0.18	0.1	0.07	0.06	0.035	0.02

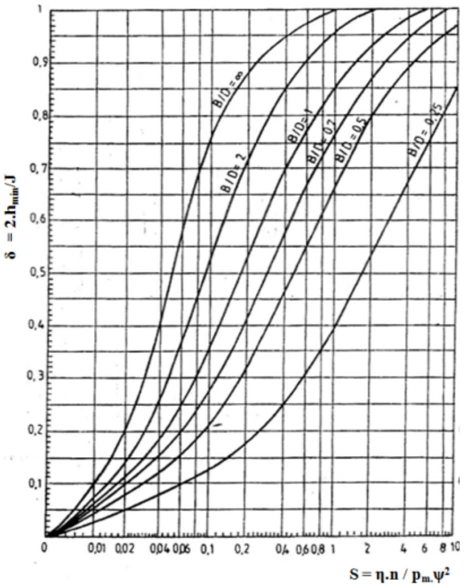

Fig. 5. Minimum relative thickness variation of the lubricant film diagram

The lubricant film minimum thickness according to relation (6) is expressed in Table 15.

Table 15

Minimum lubricant film thickness

hmin(Ψi) [μm]					
1.074	0.90375	0.73806	0.723	0.52718	0.34945
1.074	0.90375	0.73806	0.723	0.52718	0.34945
1.074	0.90375	0.73806	0.723	0.52718	0.34945
1.074	0.90375	0.73806	0.723	0.52718	0.34945
1.074	0.90375	0.73806	0.723	0.52718	0.34945
1.074	0.90375	0.73806	0.723	0.52718	0.34945

3.10 Optimal relative clearance selection

In order to be able to choose the relative optimal clearance it is necessary to make sure that we have a fluid with a sufficient thickness and a temperature that does not overheat the components. Thus, for a good functioning of the mechanism, two conditions must be met [8]:

- $T_{(\Psi i)} \leq T_{max}$
- $h_{min}(\Psi i) \geq h_{min}$

By observing the two conditions, the relatively optimal clearance is only contained in the range (0.00099...0.00175).

3.11 Minimum and maximum diametral clearance between components at T_0 temperature

We considered a steel thermal expansion coefficient $\alpha_d = 25[(°C)^{-1}]$.

$$\Psi_{min} = \Psi_1 + \alpha_d\left(T_{\Psi_1} - T_0\right) = 0.001 \quad (7)$$

$$J_{min} = d \cdot \Psi_{min} = 15.818\,[\mu m] \quad (8)$$

$$\Psi_{max} = \Psi_3 + \alpha_d\left(T_{\Psi_3} - T_0\right) = 0.002 \quad (9)$$

$$J_{max} = d \cdot \Psi_{max} = 23.457\,[\mu m] \quad (10)$$

The obtained clearance range is (15.818...23.457 microns). This arises from an approximate calculation tailored to the specific characteristics of the roller-shoe mechanism. While exploring clearance calculation models for rolling and sliding bearings, this algorithm closely aligns with the structural aspects of the mechanism.

Using this optimized clearance range, we should reduce the wear of the roller-shoe mechanism.

To validate this outcome, a running test of the roller-shoe mechanism under more aggravating conditions than the typical ones is essential.

4. EXPERIMENTAL VALIDATION FOR ROLLER-SHOE MECHANISM WITH OPTIMIZED CLEARANCE

To perform this test, we took a batch of 12 roller-shoe assemblies, already paired, from the manufacturer's stock.

We select this batch based on the clearance values set before optimization. Subsequently, from this batch, we pinpointed roller-shoe assemblies featuring comparable clearance values to the optimized ones, intending to subject them to be tested.

Table 16 displays the measured diameter values of the components within the batch of parts

Table 16

Components diameters of the pumps taken into consideration (bold writing is for the selected pumps to be tested)

Pump	Roller diameter (mm)	Shoe diameter (mm)	Clearance (mm)
1	12.0240	12.0061	0.0179
2	12.0245	12.0123	0.0122
3	12.0211	12.0061	0.0150
4	**12.0229**	**12.0078**	**0.0151**
5	12.0243	12.0123	0.0120
6	12.0244	12.0066	0.0178
7	12.0249	11.9962	0.0287
8	**12.0201**	**11.9964**	**0.0237**
9	12.0304	11.9983	0.0321
10	12.0276	11.9956	0.0320
11	12.0314	11.9964	0.0350
12	12.0309	119961	0.0348

The pumps chosen for the test have the roller and shoe mechanism with clearance values similar with optimized range extreme values. To carry out this experiment, we used the Low Sommerfeld type test [9]. The test imposed parameters are: the pump driveshaft speed (400 rpm), the rail pressure (2500 bar) and the inlet fluid temperature (120 °C). The set test duration for each pump is 30 hours. The two pumps completed the test successfully. For this case, the visual analysis of the components is the best method to highlight the defects caused by the clearance.

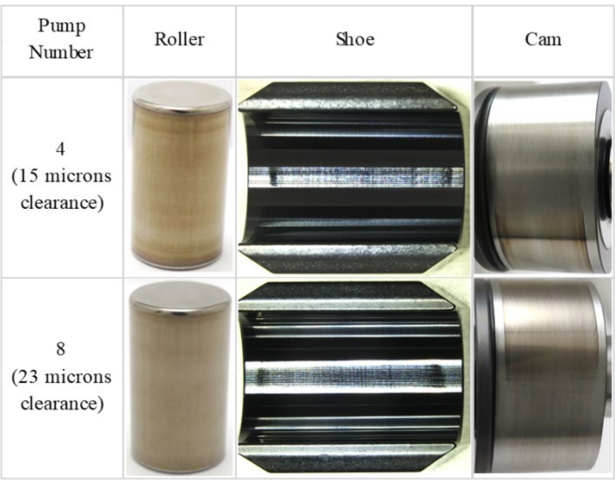

Fig. 6. Evaluation of motion-transmitting elements with optimized clearances.

Figure 6 highlights the motion transmission elements of the pumps with optimized clearance. No defects or overheated areas were observed. Upon examining the two tested pumps, we observed a visually excellent condition of the components following the optimization of roller-shoe clearance.

5. CONCLUSIONS

Increasing the life of high-pressure pumps consists in obtaining solutions to reduce the basic components wear. The computation of an ideal clearance for the roller and shoe mechanism presents a cost-effective solution. This one does not involve changes in components design or materials. Thus, following a calculation algorithm of the roller-shoe mechanism, based on real dimensional and operating information, we obtained a range of values for the optimal clearance between the components. The applicability in the industrial environment is mainly given by the reduced costs that such a modification implies. The investigation in this study relies on a strong correlation between theoretical aspects and those observed in industrial practice. The obtained result is validated by experimental tests. The test is a severe one, due to the imposed working conditions (extreme values of the working parameters). The components visual condition after the test is good. The assembly from pump 4 does not show traces of intense friction caused by the lower value of the clearance, compared to pump 8. At the same time, pump 8 did not show noises caused by component vibrations during operation, and also its transmission mechanism did not show signs of wear caused by misalignment of elements (such as longitudinal stripes on the roller). Considering these results, the obtained range of clearance can be used on the roller-shoe assembly without influencing the wear occurrence.

6. REFERENCES

[1] Horrocks, R. W., Lawther, R., Hatfield, L., 2010, *Fuel injection systems for high-speed direct injection diesel engines*, Advanced Direct Injection Combustion Engine Technologies and Development 61-104.

[2] Iordache, R. C., Petrea, N. D., Bujoreanu, C., 2020, *Wear's issues on high-pressure common rail pumps*, IOP Conference Series: Materials Science and Engineering, 724, 012021.

[3] Zabawski, E., 2014, *Lubrication Fundamental*, Society of Tribologists and Lubrication Engineers Annual Meeting & Exhibition.

[4] Wang, J., Xu, M., Zhang, C., Huang, B., Gu, F., 2020, *Online Bearing Clearance Monitoring Based on an Accurate Vibration Analysis*, Energies, 13(2), 389.

[5] Wen, B., Wang, M., Zhang, X., Zhai, J., Sun, W., 2021, *Experimental Investigation of Clearance Influences on Cage Motion and Wear in Ball Bearings*, Applied Sciences, 11(24), 11848.

[6] Liu, J., Xu, Z., An, Y., 2022, *An Analysis of the Load Distribution Characteristics of a Cylindrical Roller Bearing Including the Component Deformation and Waviness*, Journal of Tribology, 145(2).

[7] Qiu, L., Liu, S., Chen, X., Wang, Z., 2022, *Lubrication and loading characteristics of cylindrical roller bearings with misalignment and roller modifications*, Tribology International, 165, 107291.

[8] Olaru, N. D., 1993, *Tribologie. Elemente de bază asupra frecării, uzării și ungerii.*

[9] Iordache, C. R., Ciornei, F. C., Bujoreanu, C., 2019, *Scuffing analysis of roller-shoe mechanism after an aggressive test*, IOP Conference Series: Materials Science and Engineering, 591, 012020.

[10] Iordache, R. C., Petrea, N. D., Bujoreanu, C., 2022, *Study of roller-shoe contact during high-pressure injection pump normal operation*, IOP Conference Series: Materials Science and Engineering, 1235(1), 012068.

[11] Kumbár, V., Skřivánek, A., 2015, *Temperature Dependence Viscosity and Density of Different Biodiesel Blends*, Acta Universitatis Agriculturae et Silviculturae Mendelianae Brunensis, 63(4), 1147–1151.

[12] Olaru, D., 2020, *Tribologie. Cursuri cu Aplicații*, Universitatea Tehnică Gheorghe Asachi Iași, Facultatea de Mecanică.

Optimizarea jocului mecanismului rolă-sabot din pompele de înaltă presiune

Abstract: Pompa de înaltă presiune cu mecanism de transmisie cu rolă-sabot face parte din sistemul modern de alimentare cu combustibil pentru motoare diesel. Având în vedere soluția constructivă complexă și modul său de funcționare, procesul de uzură poate evolua rapid și poate duce, de asemenea, la deteriorarea catastrofală a componentelor. Mecanismul de transmisie cu rolă și sabot este subansamblul cel mai important al pompei de înaltă presiune și poate fi grav afectat de procesul de uzură. Fluidul de lucru al sistemului (motorina) este un lichid cu proprietăți tribologice slabe și este singura soluție de lubrifiere folosită în toate subansamblele pompei. Având în vedere acest lucru, este necesar să se analizeze și alți factori care pot influența condițiile tribologice ale mecanismului. Jocul diametral între componentele mecanice în contact direct este un parametru care poate avea o influență decisivă asupra procesului de uzură și, de asemenea, asupra duratei de viață a ansamblului. Cele mai relevante exemple studiate în literatură, care evidențiază condiții similare cu funcționarea sistemului cu rolă și sabot se găsesc la rulmenți. Jocul are un impact direct asupra lubrifierii între componente, asupra încălzirii acestora și, în special, a stabilității în timpul mișcării lor. Un joc mare duce la zgomot și vibrații în mecanism, iar utilizarea unui lubrifiant vâscos este recomandată. Un joc mic duce la supraîncălzirea componentelor și la formarea unui film subțire de lubrifiant. Scopul acestui articol este să efectueze un calcul analitic pentru a evidenția o gamă de valori a jocului între rolă și sabot, în care pompa de înaltă presiune poate funcționa în condiții de siguranță fără a deteriora componentele. Prin analiza vizuală și dimensională a mai multor loturi de ansamble rolă-sabot deja împerecheate din mediu industrial, s-a identificat o gamă de jocuri cu valori minime și maxime. Având în vedere acest lucru și urmând câțiva pași de bază identificați în literatură, s-a obținut un algoritm pentru a calcula jocul ideal între componente. Acesta este adaptat în funcție de geometria mecanismului, condițiile reale de funcționare și parametrii regimului de lubrifiere. Calculele sunt făcute luând în considerare funcționarea pompei de înaltă presiune în condițiile cele mai obișnuite în care regimul de lubrifiere între rolă și sabot este unul mixt. Pașii de optimizare duc la un interval mai restrâns al valorilor optime ale jocului diametral, cu beneficiul de a reduce uzura posibilă între componente.

Răzvan-Constantin IORDACHE, Assistant professor, Gheorghe Asachi Technical University of Iasi-Romania, Department of Mechanical Engineering, Mechatronics and Robotics, Blvd. Mangeron, No. 43, 700050, Iasi, Romania, constantin-razvan.iordache@academic.tuiasi.ro

Carmen BUJOREANU, Professor dr. ing. habil, Gheorghe Asachi Technical University of Iasi-Romania, Department of Mechanical Engineering, Mechatronics and Robotics, Blvd. Mangeron, No. 43, 700050, Iasi, Romania, carmen.bujoreanu@academic.tuiasi.ro

Dumitru OLARU, Prof. Em. Dr. Ing., Gheorghe Asachi Technical University of Iasi-Romania, Department of Mechanical Engineering, Mechatronics and Robotics, Blvd. Mangeron, No. 43, 700050, dumitru.olaru@academic.tuiasi.ro